

# A combined NMR- and HPLC-MS/MS-based metabolomics to evaluate the metabolic perturbations and subacute toxic effects of endosulfan on mice

Ping Zhang<sup>1,2</sup> · Wentao Zhu<sup>2</sup> · Dezhen Wang<sup>2</sup> · Jin Yan<sup>2</sup> · Yao Wang<sup>1,2</sup> · Zhiqiang Zhou<sup>2</sup> · Lin He<sup>1</sup>

Received: 6 October 2016 / Accepted: 13 June 2017 / Published online: 26 June 2017  
© Springer-Verlag GmbH Germany 2017

**Abstract** Endosulfan is the newly persistent organic pollutants (POPs) added to the Stockholm Convention as its widespread use, persistence, bioaccumulation, long-range transport, endocrine disruption, and toxicity related to various adverse effects. In the present study, male mice were administrated endosulfan at 0, 0.5, and 3.5 mg/kg by gavage for 2 weeks. <sup>1</sup>H-NMR-based urinary metabolomics, HPLC-MS/MS-based targeted serum metabolomics, clinical analysis, and histopathology techniques were employed to evaluate the metabolic perturbations of subacute endosulfan exposure. Endosulfan exposures resulted in weight loss, liver inflammation and necrosis, and alterations in serum amino acids and urine metabolomics. Based on altered metabolites, several significantly perturbed pathways were identified including glycine, serine, and threonine metabolism; TCA cycle; pyruvate metabolism; glycolysis or gluconeogenesis; glycerophospholipid metabolism; and glyoxylate and dicarboxylate metabolism. Such pathways were highly related to amino acid metabolism, energy metabolism, and lipid metabolism. In addition, metabolomic results

also demonstrated that gut microbiota was remarkably altered after endosulfan exposure. These observations may provide novel insight into revealing the potential toxic mechanism and evaluating the health risk of endosulfan exposure at metabolomic level.

**Keywords** Endosulfan · Metabolomics · Metabolic perturbation · Amino acids · <sup>1</sup>H-NMR · HPLC-MS/MS

## Introduction

Endosulfan (6,7,8,9,10,10-hexachloro-1,5,5a,6,9,9a-hexahydro-6,9-methano-2,4,3-benzodioxathiepin 3-oxide) is a widely used organochlorine pesticide in agriculture. Since its introduction as a broad spectrum insecticide in 1954, it has been extensively used on vegetables, fruits, cereal grains, cotton, and, in some cases, to preserve wood (Quinete et al. 2013; Schmidt et al. 2014). Technical endosulfan is a mixture of two isomers,  $\alpha$ -endosulfan and  $\beta$ -endosulfan, with the ratio ranging from 2:1 to 7:3 (Stanley et al. 2009). The cumulative global use of endosulfan in agriculture was estimated to 308,000 t from 1950 to 2000 (Li and Macdonald 2005). Considering its widespread use, persistence, bioaccumulation, long-range transport, endocrine disruption, and toxicity in the ecosystem, endosulfan was added to annex A of the Stockholm Convention list of persistent organic pollutants (POPs) in 2011 and phased out globally except for specific exemption (Becker et al. 2011; Weber et al. 2010). Despite the ban, endosulfan residues widely exist in different environmental matrices including soil, water, vegetables, fruit, and milk. It is reported that the surface soil concentrations of total endosulfan from 141 sites across China ranged from below detection limit to 19,000 pg/g dry weight in 2005 (Jia et al. 2010). Therefore, a deeper knowledge of metabolic perturbations and

Responsible editor: Philippe Garrigues

**Electronic supplementary material** The online version of this article (doi:10.1007/s11356-017-9534-z) contains supplementary material, which is available to authorized users.

✉ Lin He  
helinok@vip.tom.com

<sup>1</sup> Key Laboratory of Entomology and Pest Control Engineering, College of Plant Protection, Southwest University, Chongqing 400715, China

<sup>2</sup> Beijing Advanced Innovation Center for Food Nutrition and Human Health, Department of Applied Chemistry, China Agricultural University, Beijing, China

subacute toxic effects of endosulfan at metabolomic level may provide novel insight into toxic mechanism and integrative risk assessment for environment and human health.

Many studies indicated that endosulfan can induce a lot of toxic effects including neurotoxicity, genotoxicity, hepatotoxicity, cardiotoxicity, reproductive toxicity, endocrine disruption effects, and oxidative stress responses (Berntssen et al. 2008; Brunelli et al. 2009; Dorval et al. 2003; Kalender et al. 2004; Lu et al. 2000; Pereira et al. 2012; Sohn et al. 2004). Specifically, Du et al. demonstrated that endosulfan can induce reproductive dysfunction and germ cell apoptosis via regulating mitochondrial dysfunction and DNA damage response genes in *Caenorhabditis elegans* (Du et al. 2015a, b). Endosulfan can also produce reactive oxygen species (ROS) and induce DNA damage in zebrafish with dose-dependent mode (Shao et al. 2012). Yuk et al. employed NMR-based metabolomics to investigate the toxic effects of endosulfan on earthworms and found that glutamine/GABA-glutamate cycle metabolites were significantly changed, which are highly related to neurotoxicity and apoptosis induced by endosulfan (Yuk et al. 2013). Although a lot of efforts have been conducted to understand the toxicity of endosulfan, little information is available about metabolic perturbations and subacute toxic risk assessments of endosulfan on mammals, depending on much more sensitive and comprehensive metabolomic approaches.

Metabolomics is an emerging method in the field of “omics” study, which focuses on the systematic evaluation of metabolic responses of biological systems to perturbations (e.g., drug toxicity, disease, genetic variation, environmental factor, and other stimuli). Nuclear magnetic resonance (NMR) and mass spectrometry (MS) are two most commonly used techniques in metabolomic research. Environmental metabolomics is an important branch of metabolomics, which is defined as the application of metabolomic techniques to evaluate the metabolic responses of organisms to environmental stimuli, such as temperature, humidity, illumination intensity, and environmental pollutants (Aliferis and Chrysai-Tokousbalides 2011; Bundy et al. 2009; Gao et al. 2014). Integrated environmental metabolomics is powerful to investigate the metabolic perturbations and subacute toxic effects of environmental pollutants, and can provide comprehensive information for toxicity risk assessment. For example, metabolomic study can not only find potential biomarkers but also identify critical toxicity-related pathways, which are essential to reveal possible toxicity mechanism of environment contaminants.

The aim of this study was conducted to evaluate the metabolic perturbations and subacute toxic effects of endosulfan on mice using  $^1\text{H-NMR}$ - and HPLC-MS/MS-based metabolomic approaches.  $^1\text{H-NMR}$ -based metabolomic profile, HPLC-MS/MS-based targeted detection, multivariate pattern recognition, clinical chemistry, and histopathology were determined

on mice after endosulfan exposure for 2 weeks. Integrated analyses were investigated on all obtained data to systematically identify altered molecular pathways and mechanism of toxicological effects. To our knowledge, this is the first systematic metabolic perturbations and toxic analysis of endosulfan on mice at molecular level using mouse urine metabolomics.

## Materials and methods

### Chemical and materials

Endosulfan (purity  $\geq 98.0\%$ ) was purchased from Jiangsu Kuaida Agrochemical Co., Ltd. (Nantong, China). Deuterium oxide ( $\text{D}_2\text{O}$ ; 99.9% D) and sodium 3-trimethylsilyl [2,2,3,3- $^2\text{H}_4$ ] propionate (TSP) were bought from Cambridge Isotope Laboratories, Inc. (Tewksbury, MA, USA). Unlabeled amino acids and [ $^{13}\text{C}$ ,  $^{15}\text{N}$ ] labeled cell-free amino acid mixture were purchased from Sigma-Aldrich (St. Louis, MO, USA).  $\text{K}_2\text{HPO}_4 \cdot 3\text{H}_2\text{O}$  and  $\text{NaH}_2\text{PO}_4 \cdot 2\text{H}_2\text{O}$  were bought from Sinopharm Chemical Co., Ltd. (Beijing, China). Solvents for sample preparation and HPLC-MS/MS analysis were HPLC grade and purchased from Fisher Chemicals (Beijing, China). Ultrapure water was generated by a Milli-Q system from Millipore (Billerica, MA, USA). Other reagents were analytical grade and purchased from Sinopharm Chemical Reagent Co., Ltd. (Beijing, China).

### Animals and animal treatments

Eight-week-old male mice (*Mus musculus*, ICR) were purchased from the Vital River Laboratory Animal Company (Beijing, China). The male *M. musculus* mice were chosen for the sensitive response to xenobiotic exposure in environmental research (Zhang et al. 2013). Animals were acclimated for 2 weeks before being transferred to metabolic cages. During the experiment, mice were housed at  $25 \pm 3^\circ\text{C}$ ,  $50 \pm 5\%$  relative humidity, and 12/12-h light/dark cycle with free access to water and food. A total of 18 mice were randomly assigned to 3 groups, including control group (C; vehicle corn oil,  $n = 6$ ), low-dose group (L; 0.5 mg/kg b.w.,  $n = 6$ ), and high-dose group (H; 3.5 mg/kg b.w.,  $n = 6$ ). The low-dose concentration was derived from no observable adverse effect level in the acute oral rat neurobehavioral toxicity test (0.7 mg/kg) reported by California Department of Pesticide Regulation (CDPR) (Silva and Beauvais 2010). High-dose concentration was mainly based on hepatotoxicity and reproductive toxicity test of endosulfan in mice (5 mg/kg) reported by previous studies (Guo et al. 2016; Uboh et al. 2011). Endosulfan was suspended in corn oil and given to mice by gavage daily for 2 weeks. Urine samples were

collected every 24 h and body weights were also recorded daily. At the end of feeding trails, blood was collected into Na-heparin tubes from the eye, and plasma samples were obtained after centrifugation. Serum samples for clinical biochemistry assays were also collected when the mice were sacrificed after anesthesia. Sections of liver were taken and stored in formalin solution for histological assessments. All animal experiments were performed in accordance with the NIH guide for the care and use of laboratory animals and approved by the independent Animal Ethical Committee of China Agricultural University.

### Clinical biochemistry and histopathology

Clinical biochemistry parameters including albumin (ALB), alanine aminotransferase (ALT), aspartate aminotransferase (AST), alkaline phosphatase (ALP), blood urea nitrogen (BUN), and creatinine (Crea) were analyzed by HITACHI 7080 automatic analyzer (Hitachi, Ltd.). Liver tissues were fixed in 10% formalin for at least 12 h, and cut into 4  $\mu\text{m}$  paraffin sections. Liver slides were stained with hematoxylin and eosin (H&E) and observed under a microscope.

### $^1\text{H-NMR}$ spectroscopy analysis

Of the phosphate sodium buffer (0.2 M  $\text{NaH}_2\text{PO}_4$  and 0.2 M  $\text{K}_2\text{HPO}_4$ , pH = 7.4), 200  $\mu\text{L}$  was added to 400  $\mu\text{L}$  of urine sample collected on the 14th day to minimize variations in the pH of the urine. The mixture was homogenized and centrifuged at 4000 rpm for 10 min at 4  $^\circ\text{C}$  to remove any precipitates. Of the aliquots of supernatant from each urine sample, 500  $\mu\text{L}$  was added with 50  $\mu\text{L}$  TSP/ $\text{D}_2\text{O}$  (3 mM final concentration) and transferred into 5-mm NMR tubes for analysis. TSP acted as a chemical shift reference ( $\delta = 0.00$  ppm) and  $\text{D}_2\text{O}$  provided a lock signal. Water signals were suppressed by presaturation.

$^1\text{H-NMR}$  spectra of all samples were acquired using a Bruker AV600 spectrometer (Bruker Co., Germany) at 298 K. For each urine sample, the spectrum was acquired with a standard pulse sequence (nuclear overhauser enhancement spectroscopy (NOESY)) using 64 free induction decay (FID), 64-k data points. The FIDs were weighted by an exponential function with a 0.3-Hz line-broadening factor prior to Fourier transformation. After Fourier transformation, the phase and baseline of the spectra were manually corrected using MestReNova software. All the spectra were referenced to TSP ( $\delta = 0.00$  ppm). Each spectrum was segmented into 0.02-ppm chemical shift bins corresponding to the range from 0.20 to 10 ppm. The region at 4.50–6.00 ppm was excluded to remove the effects of imperfect water suppression efficiency and urea signal. Then, all remaining regions were scaled to the total integrated area of the spectra to facilitate comparison among the samples.

Multivariate data analysis was performed with the software package SIMCA-P (v11.0, Umetrics, Sweden). Principal component analysis (PCA) was conducted using the mean-centered data to generate an overview for group clustering and search for possible outliers. Partial least squares discriminant analysis (PLS-DA) was used to explore the main effects in the NMR data set. The metabolites were identified according to HMDB database and previous studies (An et al. 2013; Dong et al. 2013; Li et al. 2013). Significantly changed metabolites were identified on one-way analysis of variance (ANOVA) and the variable influence on project score (VIP > 1).

### HPLC-MS/MS analysis

All the samples were analyzed by an API 2000 tandem mass spectrometer (AB Sciex Instruments, Foster, CA), equipped with a polarity interchangeable electrospray Turbo Ion Spray source. The mass spectrometer was operated using Analyst software (version 1.4.2, Applied Biosystems, Foster, CA). Multiple reaction monitoring (MRM) and positive ion mode were used for detection (Table S2). The optimized MS/MS conditions were as follows: ion spray voltage (IS) at 5000 V, curtain (CUR) gas pressure at 10 psi, gas 1 (GS1) at 45 psi, gas 2 (GS2) pressure at 50 psi, ion spray source temperature at 450  $^\circ\text{C}$ , and collision gas at medium. Chromatography was conducted on an Agilent 1200 series HPLC (Agilent, Santa Clara, CA) equipped with G1322A degasser, G1311A pump, and G1329A ALS. A Phenomenex EZfaast C18 column (250  $\times$  2.0 mm, 4  $\mu\text{m}$ ) column equipped with a guard cartridge system was used to determine amino acids with mobile phase A (0.1% formic acid in water, v/v) and B (0.1% formic acid in acetonitrile, v/v). The gradient was shown in Table S1. The sample preparation and detection method were according to the previous study (Kaspar 2009).

### Biological pathway analysis

Typically, an integrative analysis based on the significantly changed metabolites was performed to explain the major perturbed biological pathways induced by endosulfan exposure. In this study, metabolic pathway perturbations were conducted by MetaboAnalyst 3.0 (<http://www.metaboanalyst.ca/>) and related metabolic pathway profiles were determined based on Kyoto Encyclopedia of Genes and Genomes (KEGG) pathway database (<http://www.kegg.jp/kegg/pathway.html>).

### Statistical analysis

One-way ANOVA was used to evaluate the statistical differences of biological parameters between treated groups and control group. All analyses were performed using SPSS 13.0 software (SPSS Inc., USA). A value of  $p < 0.05$  was considered significant.

## Results

### Phenotypes, histopathology, and clinical biochemistry of animal models

After 2 weeks of exposure, no death was observed in all groups. Figure S1 displays the average body weight of control group and two treatment groups on 1, 3, 5, 7, 10, and 14 days. It showed that significant changes ( $p < 0.05$ ) were only observed in high-dose treated group, and no obvious body weight changes were founded between control and low-dose treated group. Histopathological observation indicated that endosulfan induced inflammation and necrosis in mouse liver even in low-dose treatment (Fig. 1). Such results clearly suggested that endosulfan can induce liver injury in mice. Blood biochemical results showed the increased level of ALT and decreased level of ALP in high-dose treatment group compared with the control group ( $p < 0.05$ ). There were no significant changes in other biochemical parameters in all groups (Table 1).

### Metabolomic alteration induced by endosulfan exposure

In this study, metabolic profile of urine was determined by  $^1\text{H-NMR}$ . Figure S2 shows the representative  $^1\text{H-NMR}$  spectrums of urine samples collected from control group, low-dose treated group, and high-dose treated group, respectively. After PCA analysis, no outliers were observed in control group and two treated groups. In order to further investigate the global urine metabolic profile changes in mice after treated with endosulfan, a supervised PLS-DA was adopted to visualize the group clustering based on  $^1\text{H-NMR}$  data sets. Figure 2 presents PLS-DA plot and corresponding loading plot between treated groups and control group. PLS-DA results revealed that the low-dose treated group and high-dose treated group were clearly separated with control group, suggesting that the urine metabolic profiles of mice were obviously disturbed by endosulfan after 2 weeks of consecutive exposure. Generally, the fitness and prediction capabilities of

PLS-DA mode were assessed by  $R^2X$ ,  $R^2Y$ , and  $Q^2$ , respectively. High  $R^2Y$  leads to a high  $Q^2$  value and a robust mode was referred to a  $Q^2 > 0.4$  (McCombie et al. 2009). As shown in Fig. 2, the values of  $R^2X$ ,  $R^2Y$ , and  $Q^2$  were acceptable with  $Q^2 = 0.403$  and  $Q^2 = 0.613$ , respectively, indicating an excellent predictive capability of PLS-DA. The loading plots generated from PLS-DA mode were shown in Fig. 2c, d, which was plotted to get the discriminate variables. Based on the VIP values ( $\text{VIP} > 1$ ) and ANOVA results ( $p < 0.05$ ), a total of 18 metabolites were finally identified in mouse urine metabolic profile based on HMDB database and previous studies (An et al. 2013; Dong et al. 2013; Li et al. 2013). Low-dose endosulfan treatment group induced increased levels of alanine, pyruvate, succinate, citrate, DMA, dimethylglycine, choline, and TMAO and decreased levels of acetate, PC, GPC, scyllo-inositol, glycine, hippurate, formate, and nicotinamide. High-dose endosulfan treatment induced upregulated levels of lactate, pyruvate, succinate, and TMAO and downregulated levels of acetate, glucose, glycine, hippurate, formate, and nicotinamide in mouse urine. Furthermore, some metabolite fluctuations were dose-dependent such as lactate, acetate, DMA, and glucose (Table 2).

### Biological pathways affected by endosulfan exposure

Metabolomic profiling can not only reveal the alteration of individual metabolites but also provide a comprehensive view of metabolic process induced by toxic exogenous compounds. In the present study, MetaboAnalyst 3.0 was employed to reveal the major perturbed pathways based on significantly changed metabolites in mouse urine induced by endosulfan (Fig. 3). As a result, six metabolic pathways were filtered out as potential target pathways, including glycine, serine, and threonine metabolism; TCA cycle; pyruvate metabolism; glycolysis or gluconeogenesis; glycerophospholipid metabolism; and glyoxylate and dicarboxylate metabolism. Those pathways were highly related to amino acid metabolism, lipid metabolism, and energy metabolism.

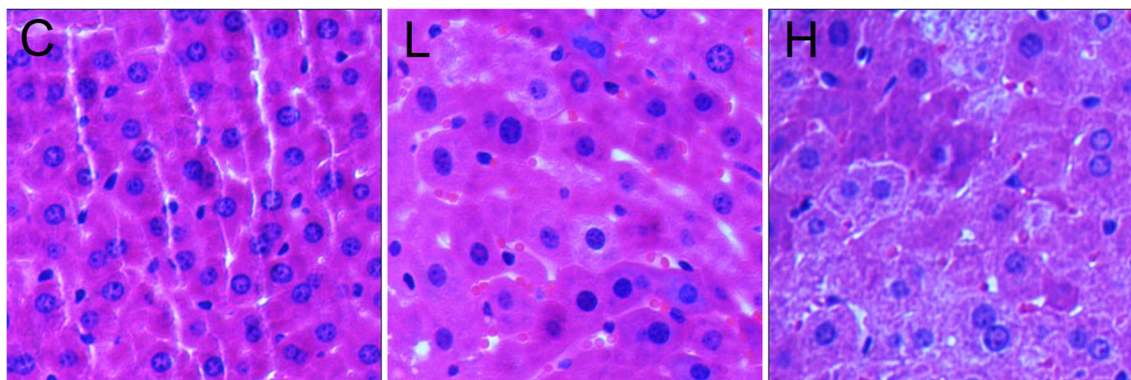


**Fig. 1** Representative histopathological sections of liver after treated with endosulfan (C) control group, (L) low-dose group, and (H) high-dose group

**Table 1** Clinical parameters of mice after orally treated with endosulfan for 2 weeks

Parameters	Control	Low dose	High dose
ALT (U/L)	22.2 ± 5.4	26.2 ± 2.7	28.7 ± 1.9*
AST (U/L)	115.0 ± 13.5	111.8 ± 16.5	108.6 ± 17.2
ALB (g/L)	32.5 ± 1.3	31.4 ± 2.6	33.3 ± 1.2
ALP (IU/L)	153.0 ± 14.9	150.8 ± 19.3	137.3 ± 10.1*
BUN (mmol/L)	8.1 ± 0.5	8.8 ± 2.0	9.7 ± 2.7
CRE (μmol/L)	28.4 ± 1.8	29.9 ± 3.3	29.4 ± 0.9

Data were presented as mean ± SD. Statistical analysis was performed by one-way ANOVA

ALT alanine aminotransferase, AST aspartate aminotransferase, ALB albumin, ALP alkaline phosphatase, BUN blood urea nitrogen, CR creatinine

\* $p < 0.05$  indicates statistically significant differences relative to the control group

### Amino acid changes in serum after endosulfan exposure

Serum amino acids were accurately quantitated using stable isotope-labeled internal standards by HPLC-MS/MS (Fig. 5 and Fig. S3). Stable isotope-labeled amino acids contribute to correcting the chromatogram shift in detection and simplify sample preparation procedures. Figure S3 shows the representative chromatograms of amino acids, and the linearities of 20 amino acids are good with all the coefficient of correlation

above 0.99. As a consequence, the levels of threonine and tryptophan decreased after low-dose endosulfan treatment. However, 10 amino acids were significantly changed after high-dose endosulfan exposure, including alanine, glutamine, glutamic acid, lysine, phenylalanine, proline, threonine, tryptophan, tyrosine, and valine (Figs. 4 and 5). Furthermore, targeted amino acid detection showed that endosulfan perturbed serum amino acid metabolism in a dose-dependent manner; with increasing dose of endosulfan, the concentration of amino acids decreased significantly.

## Discussion

### Histopathology and clinical biochemistry study

After exposure to endosulfan at two concentrations for 2 weeks, hepatocellular inflammation and necrosis were clearly observed through histopathology investigation. Such results were also confirmed by serum biochemistry analysis. Serum ALT, AST, ALB, ALP, BUN, and CRE were used as clinical indicators for liver injury. The increased level of ALT and decreased level of ALP in treated group indicated that endosulfan can lead to liver dysfunction. Liver is the main and essential organ for metabolism and detoxification of xenobiotics in mammal. In addition, hepatotoxicity and liver

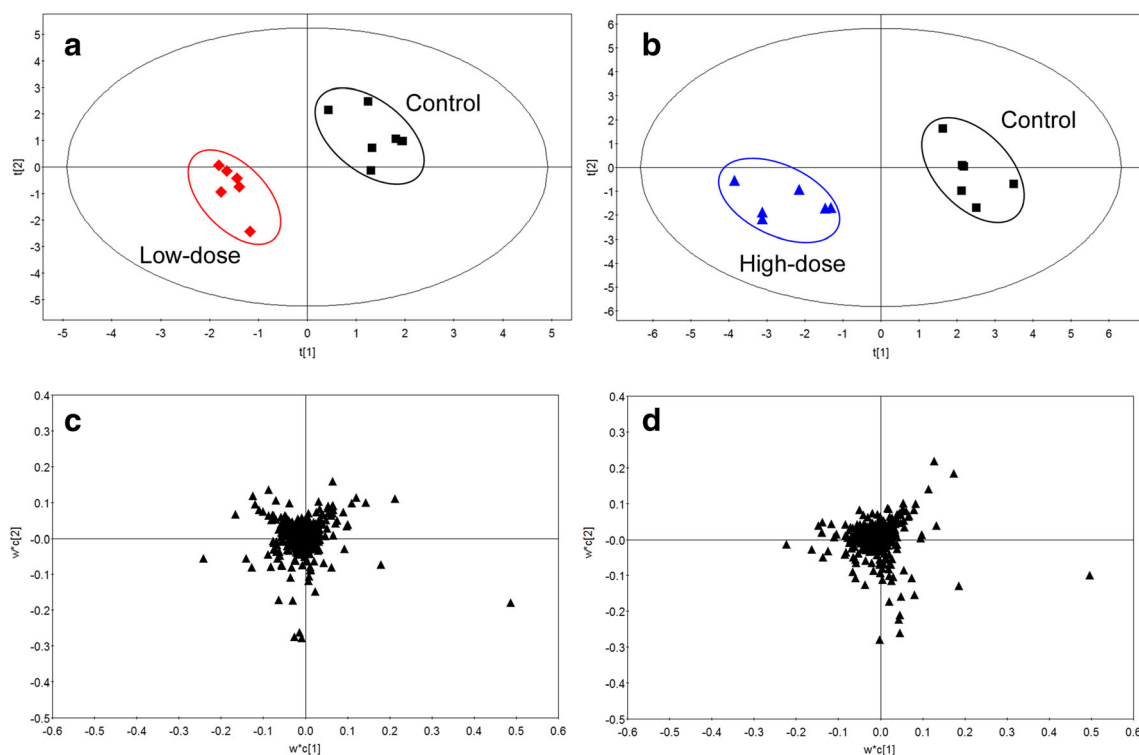


**Fig. 2** Partial least squares discriminant analysis (PLS-DA) based on urine  $^1\text{H-NMR}$  spectra. **a** Low-dose group (red diamond) versus control group (black square) ( $R^2X = 0.535$ ,  $R^2Y = 0.977$ ,  $Q^2 = 0.403$ ). **b** High-dose group (blue triangle) versus control group (black square)

( $R^2X = 0.629$ ,  $R^2Y = 0.982$ ,  $Q^2 = 0.613$ ). **c** Loading plot from low-dose group versus control group. **d** Loading plot from high-dose group versus control group

**Table 2** Alterations of urine metabolites induced by endosulfan treatment

Metabolites	HMDB ID	Chemical shift δH ppm (multiplicity <sup>a</sup> , moiety)	VIP	Fold change		Trend
				Low dose	High dose	
Lactate	HMDB00190	1.33(d, CH <sub>3</sub> ); 4.11(q, CH)	1.69	0.91	1.15*	Up
Alanine	HMDB00161	1.46(d, CH <sub>3</sub> ); 3.78(q, CH)	3.58	1.50*	1.26	Up
Acetate	HMDB00042	1.92(s, CH <sub>3</sub> )	9.30	0.86*	0.74*	Down
Pyruvate	HMDB00243	2.37(s, CH <sub>3</sub> )	1.87	1.26*	1.12*	Up
Succinate	HMDB00254	2.41(s, CH)	4.28	1.18*	1.06*	Up
Citrate	HMDB00094	2.54(d, CH <sub>2</sub> ); 2.67(d, CH <sub>2</sub> )	2.57	1.22*	1.03	Up
DMA	HMDB00087	2.72(s, CH <sub>3</sub> )	1.81	1.11*	1.23	Up
Dimethylglycine	HMDB00092	2.93(s, CH <sub>3</sub> ); 3.73(s, CH <sub>2</sub> )	1.67	1.17*	0.93	Up
Choline	HMDB00097	3.21(s, CH <sub>3</sub> ); 3.52(m, N-CH <sub>2</sub> ); 4.07(m, O-CH <sub>2</sub> )	1.73	1.27*	1.29	Up
PC	HMDB01565	3.22(s, CH <sub>3</sub> ); 3.59(m, N-CH <sub>2</sub> ); 4.17(m, O-CH <sub>2</sub> )	2.74	0.65*	0.72	Down
GPC	HMDB00086	3.23(s, CH <sub>3</sub> ); 3.68(m, N-CH <sub>2</sub> ); 3.69(m, O-CH <sub>2</sub> ); 4.33(m, P-O-CH <sub>2</sub> )	2.07	0.45*	0.73	Down
TMAO	HMDB00925	3.27(s, CH <sub>3</sub> )	1.58	1.76*	1.51*	Up
Scyllo-inositol	HMDB06088	3.35(s, CH)	1.49	0.45*	0.58	Down
Glucose	HMDB00122	3.25(dd, CH); 3.41(t, CH); 3.46(m, CH); 3.49(t, CH); 3.72(dd, CH); 3.90(dd, CH); 4.65(d, CH)	1.24	0.98	0.84*	Down
Glycine	HMDB00123	3.52(s, CH <sub>2</sub> )	2.09	0.93*	0.96	Down
Hippurate	HMDB00714	3.97(d, CH <sub>2</sub> ); 7.55(t, CH); 7.64(t, CH); 7.84(d, CH)	1.62	0.91*	0.96	Down
Formate	HMDB00142	8.46(s, CH)	4.37	0.74*	0.77*	Down
Nicotinamide	HMDB01406	7.59(dd, CH); 8.24(dd, CH); 8.72(dd, CH); 8.94(s, CH)	1.49	0.65*	0.75*	Down

DMA dimethylamine, PC phosphorylcholine, GPC glycerophosphocholine, TMAO trimethylamine N-oxide

<sup>a</sup> s, singlet; d, doubles; t, triples; m, multiplets; q, quartet; dd, double doublet

\**p* < 0.05 (one-way ANOVA)

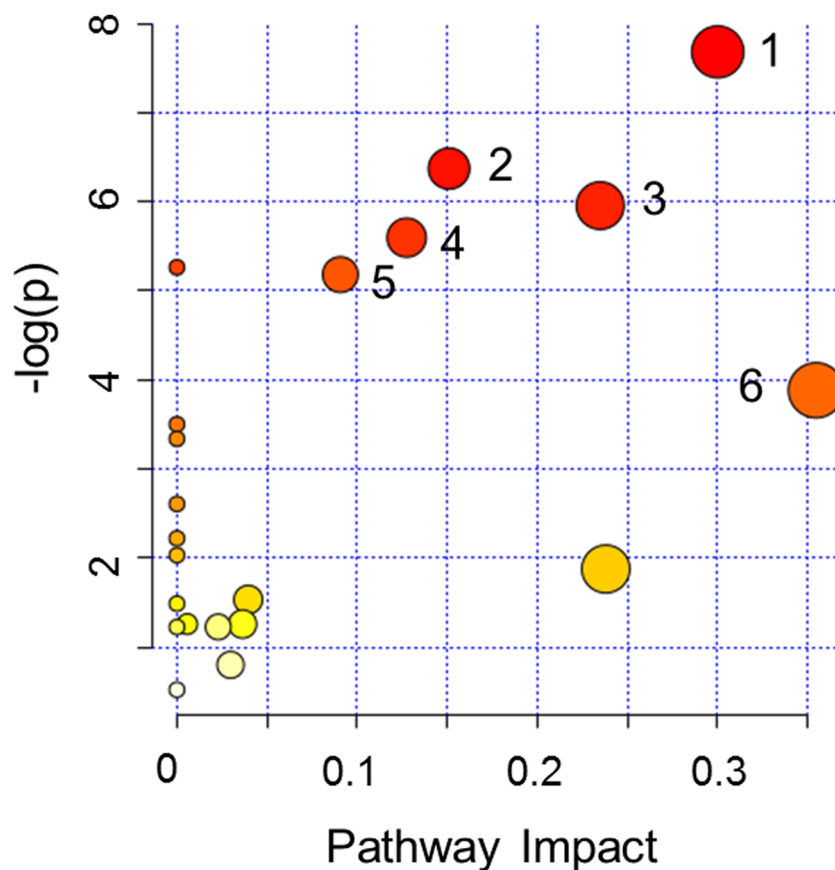
dysfunction induced by POPs have been widely verified (Machala et al. 2004; Noel et al. 2014; Nomiya et al. 2014; Shi et al. 2012; Song et al. 2015).

**Amino acid metabolism**

In the present study, urine metabolomic results revealed that amino acid metabolisms were significantly perturbed due to endosulfan exposure, including glycine, serine, and threonine metabolism (Fig. 6). Amino acids and their metabolites play vital roles in humans and animals, which not only build blocks of polypeptide and proteins but also are critical for growth, maintenance, reproduction, and immunity in mammal (Landfried et al. 2011; van der Goot et al. 2012; Wu 2009; Zhu et al. 2011). Figure 6 indicates that endosulfan caused the increased of alanine and decreased of glycine in mouse urine. Alanine is a non-essential amino acid and can inhibit L-type pyruvate kinase, thus regulating gluconeogenesis and glycolysis to ensure glucose production by hepatocytes (Meijer 2003;

Xu et al. 2015). Glycine is an inhibitory neurotransmitter in the central nervous system, and its product glutathione is the major antioxidant in cells and regulates the homeostasis of free radical (Amelio et al. 2014; Mehrmohamadi et al. 2014; Wu et al. 2004). Furthermore, targeted serum HPLC-MS/MS analysis indicated that alanine, glutamine, glutamic acid, lysine, phenylalanine, proline, threonine, tryptophan, tyrosine, and valine decreased in serum after endosulfan exposure. These amino acids regulate specific pathway and have different functions in humans and animals. For example, tyrosine and phenylalanine are the precursors for the synthesis of dopamine, norepinephrine, epinephrine, and thyroid hormones, which are important for neurological development (Wu 2009). Much evidence also shows that amino acids including alanine, glutamine, glutamic acid, lysine, phenylalanine, and glycine participate in cell-specific metabolism of nutrients, cell signaling, and oxidative stress (Jobgen et al. 2006; Mannick 2007; Marc Rhoads and Wu 2009). Tryptophan, glutamine, proline, and methionine play important roles in

**Fig. 3** Summary of pathway analysis with MetaboAnalyst 3.0. 1 Glycine, serine, and threonine metabolism. 2 TCA cycle. 3 Pyruvate metabolism. 4 Glycolysis or gluconeogenesis. 5 Glycerophospholipid metabolism. 6 Glyoxylate and dicarboxylate metabolism



enhancing the immune function of mammal. Specifically, metabolism of tryptophan via kynurenine pathway by indoleamine-2,3-dioxygenase is highly related to graft-versus-host disease, age-related neurological diseases, immunological diseases, and cancer (Favre et al. 2010; Hiruma et al. 2013).

### Energy metabolism

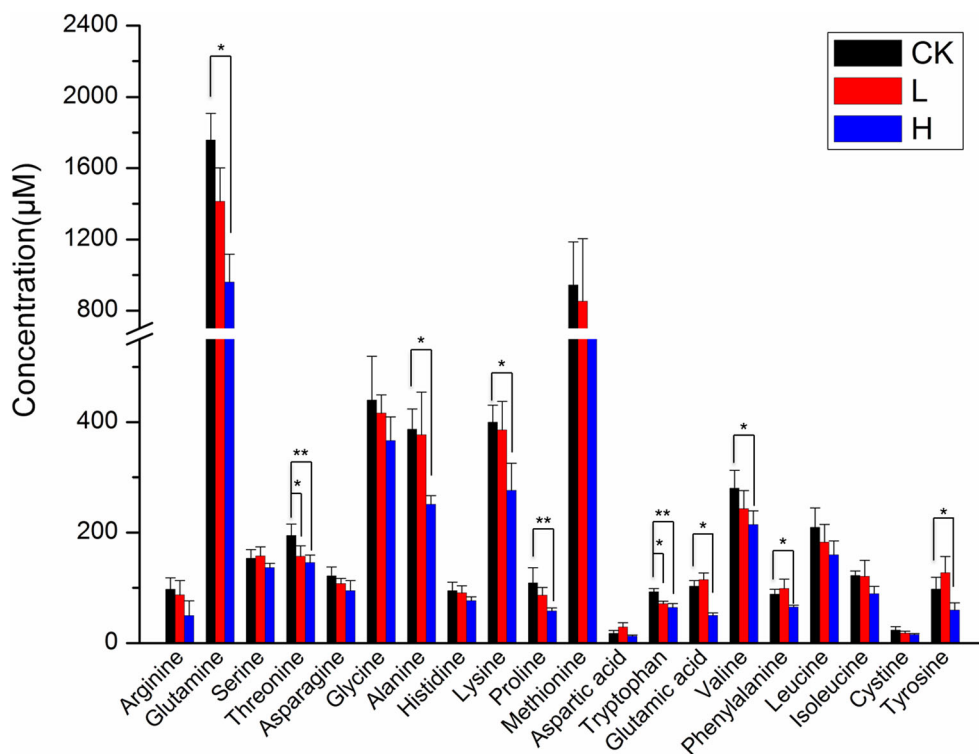
Energy metabolism-related metabolites including citrate, succinate, pyruvate, alanine, and lactate were significantly perturbed in mouse urine after endosulfan exposure. Citrate and succinate are the main intermediates of the TCA cycle, a vital energy production pathway in cells; pyruvate metabolism-related metabolites including pyruvate, alanine, and lactate are also essential for energy metabolism. Furthermore, pyruvate is an important product of glycolysis and can be converted into acetyl-CoA, which is an important precursor for citrate synthesis. Thus, the increased levels of citrate, succinate, pyruvate, alanine, and lactate clearly indicate that energy metabolism-related pathways including TCA cycle and pyruvate metabolism were significantly affected by endosulfan exposure. Another good example for the perturbation of energy metabolism was the downregulated

acetate in urine after endosulfan exposure. Acetate is an end product of fatty acid oxidation, and the decreased level of acetate in mouse urine clearly indicates the perturbed  $\beta$ -oxidation of fatty acids, which may result in affecting energy metabolism after endosulfan exposure.

### Lipid metabolism

Based on metabolomic results, glycerophospholipid metabolism metabolites such as choline, PC, GPC, and acetate were significantly changed after endosulfan exposure. The downregulated PC, GPC, and acetate and upregulated choline obviously indicate the perturbed of lipid metabolism. Choline, PC, and GPC are known to be important endogenous compounds required for cell and mitochondrial membranes, neurotransmitter synthesis, methylation-dependent biosynthesis, lipid transportation, and bile acid secretion (Al Rajabi et al. 2014; Kohlmeier et al. 2005; Trousil et al. 2014). Evidence shows that choline metabolite deficiency contributes to various disorders in humans and animals, including fatty liver development, liver cell death, skeletal muscle damage, liver steatosis and hepatocarcinogenesis, and mitochondrial dysfunction (Li et al. 2005; Zeisel 2011; Zhu et al. 2014). PC and GPC

**Fig. 4** Alteration of serum amino acids induced by endosulfan

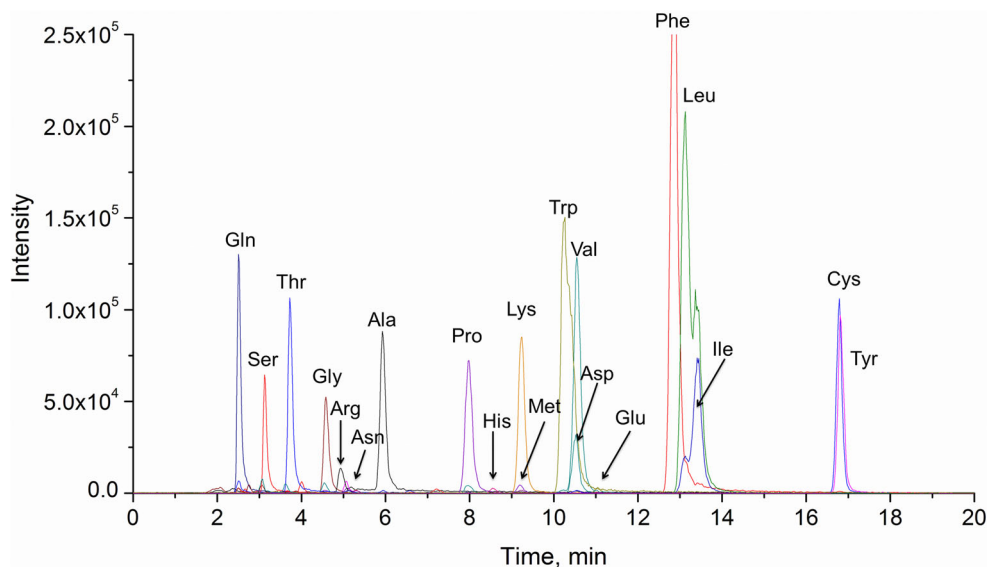


can not only maintain choline homeostasis but also protect cells and their organelles from oxidative stress and inflammation (Bollard et al. 2010; Zhang et al. 2011, 2014, 2015a). Considering that the main choline metabolism occurred in liver, the increased level of choline and decreased level of PC and GPC may also reflect the dysfunction of liver metabolism after endosulfan exposure. Such results are consistent with our previous histopathology and clinical biochemistry study.

**Gut microbiota changes induced by endosulfan**

Hippurate is the most widely detected metabolite in urine and formed by the conjugation of glycine with benzoate in the liver of mammals (Tyagi et al. 2012; Zhang et al. 2015b). Benzoate is mainly derived from aromatic acids or plant phenolics by the action of gut microbiota (Wang et al. 2012). As a result, hippurate concentration is highly related to gut microbial composition and activity. The level of hippurate

**Fig. 5** Representative LC-MS/MS chromatogram of amino acids





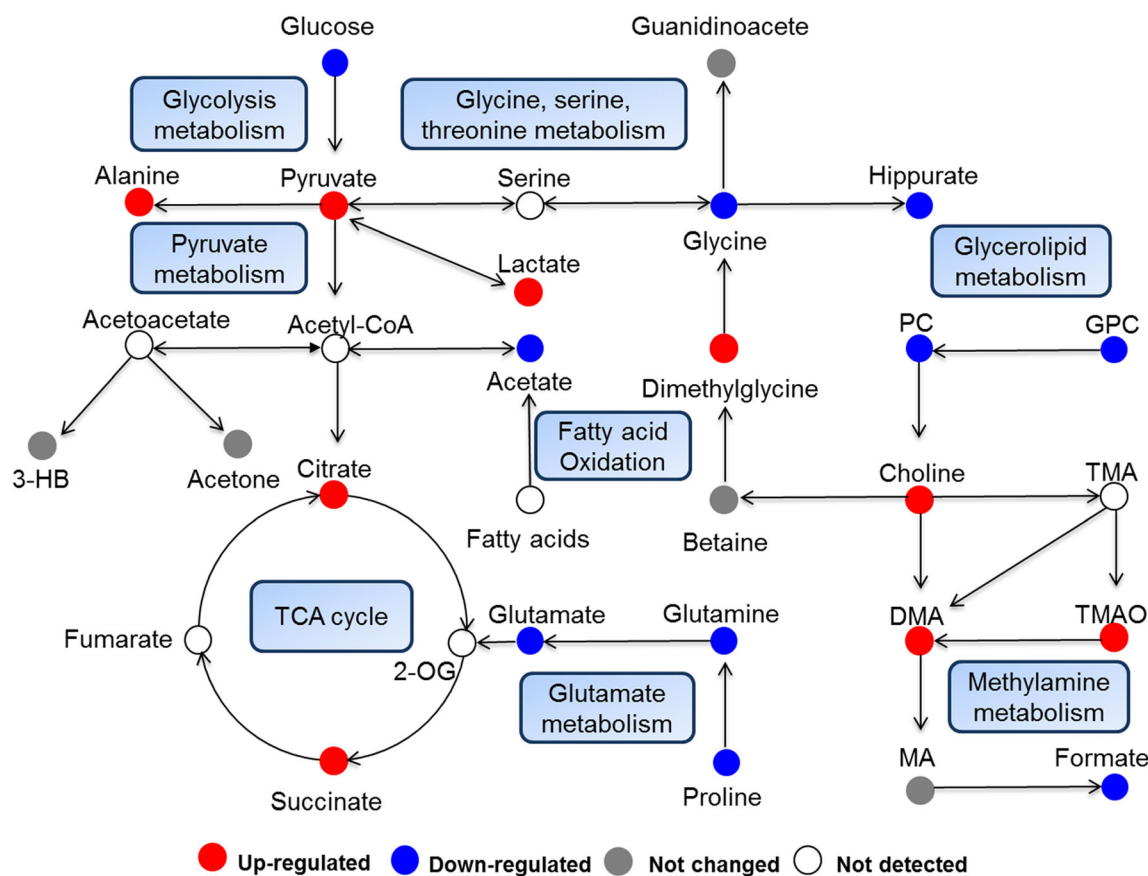


**Fig. 6** Perturbed pathways and fluctuant metabolites induced by endosulfan exposure

decreased after endosulfan exposure in mice, which clearly indicated the alteration in gut microbiota. Combining the results of amino acids, the decreased level of hippurate may be result from glycine decrease in mouse urine after endosulfan exposure. Another metabolism pathway affected by gut microbiota is choline metabolism. Choline can be metabolized to TMA, DMA, TMAO, and MA by gut microbiota. Here, we observed the increased levels of choline, DMA, and TMAO in mice after endosulfan exposure. Furthermore, the gut microbiota-associated alteration of choline may also affect the conversion of choline to other metabolites, such as betaine, dimethylglycine, glycine, hippurate, and guanidinoacetate. To sum up, the alteration of hippurate and choline metabolism pathways indicated that endosulfan induced gut microbial colony changes in mice; such fluctuation may affect absorption of nutrient from diet and hence the growth of the mice.

## Conclusion

This study represents metabolic perturbations and subacute toxic effects of mice exposed to endosulfan using HPLC-MS/MS- and  $^1\text{H-NMR}$ -based metabolomics. Our results indicate that endosulfan exposure induced liver injury, disruption of amino acid metabolism, lipid metabolism, energy

metabolism, and gut microbiota metabolism. In conclusion, this study illustrates that HPLC-MS/MS- and  $^1\text{H-NMR}$ -based metabolomic approaches are sensitive and suitable for monitoring the systematic metabolic effects of endosulfan exposure on mice, which can provide integrative information for the potential toxic mechanism and evaluate the health risk of endosulfan exposure at molecular level.

**Acknowledgements** This study was financially supported by the National Natural Science Foundation of China (21207158, 21337005).

## Compliance with ethical standards

**Conflict of interest** The authors declare that they have no conflict of interest.

## References

- Al Rajabi A et al (2014) Choline supplementation protects against liver damage by normalizing cholesterol metabolism in *Pemt/Ldlr* knockout mice fed a high-fat diet. *J Nutr* 144:252–257. doi:10.3945/jn.113.185389
- Aliferis KA, Chrysai-Tokousbalides M (2011) Metabolomics in pesticide research and development: review and future perspectives. *Metabolomics* 7:35–53. doi:10.1007/s11306-010-0231-x

- Amelio I, Cutruzzola F, Antonov A, Agostini M, Melino G (2014) Serine and glycine metabolism in cancer. *Trends Biochem Sci* 39:191–198. doi:10.1016/j.tibs.2014.02.004
- An Y et al (2013) High-fat diet induces dynamic metabolic alterations in multiple biological matrices of rats. *J Proteome Res* 12:3755–3768. doi:10.1021/pr400398b
- Becker L, Scheringer M, Schenker U, Hungerbühler K (2011) Assessment of the environmental persistence and long-range transport of endosulfan. *Environ Pollut* 159:1737–1743. doi:10.1016/j.envpol.2011.02.012
- Berntssen MH, Glover CN, Robb DH, Jakobsen JV, Petri D (2008) Accumulation and elimination kinetics of dietary endosulfan in Atlantic salmon (*Salmo salar*). *Aquat Toxicol* 86:104–111. doi:10.1016/j.aquatox.2007.10.006
- Bollard ME et al (2010) NMR-based metabolic profiling identifies biomarkers of liver regeneration following partial hepatectomy in the rat. *J Proteome Res* 9:59–69. doi:10.1021/pr900200v
- Brunelli E, Bernabo I, Berg C, Lundstedt-Enkel K, Bonacci A, Tripepi S (2009) Environmentally relevant concentrations of endosulfan impair development, metamorphosis and behaviour in *Bufo bufo* tadpoles. *Aquat Toxicol* 91:135–142. doi:10.1016/j.aquatox.2008.09.006
- Bundy JG, Davey MP, Viant MR (2009) Environmental metabolomics: a critical review and future perspectives. *Metabolomics* 5:3–21. doi:10.1007/s11306-008-0152-0
- Dong F, Zhang L, Hao F, Tang H, Wang Y (2013) Systemic responses of mice to dextran sulfate sodium-induced acute ulcerative colitis using <sup>1</sup>H NMR spectroscopy. *J Proteome Res* 12:2958–2966. doi:10.1021/pr4002383
- Dorval J, Leblond VS, Hontela A (2003) Oxidative stress and loss of cortisol secretion in adrenocortical cells of rainbow trout (*Oncorhynchus mykiss*) exposed in vitro to endosulfan, an organochlorine pesticide. *Aquat Toxicol* 63:229–241. doi:10.1016/s0166-445x(02)00182-0
- Du H et al (2015a) Endosulfan isomers and sulfate metabolite induced reproductive toxicity in *Caenorhabditis elegans* involves genotoxic response genes. *Environ Sci Technol* 49:2460–2468. doi:10.1021/es504837z
- Du H et al (2015b) Reproductive toxicity of endosulfan: implication from germ cell apoptosis modulated by mitochondrial dysfunction and genotoxic response genes in *Caenorhabditis elegans*. *Toxicol Sci* 145:118–127. doi:10.1093/toxsci/kfv035
- Favre D et al (2010) Tryptophan catabolism by indoleamine 2,3-dioxygenase 1 alters the balance of TH17 to regulatory T cells in HIV disease. *Sci Transl Med* 2:32ra36. doi:10.1126/scitranslmed.3000632
- Gao Y et al (2014) Identifying early urinary metabolic changes with long-term environmental exposure to cadmium by mass-spectrometry-based metabolomics. *Environ Sci Technol* 48:6409–6418. doi:10.1021/es500750w
- Guo FZ et al (2016) Endosulfan inhibiting the meiosis process via depressing expressions of regulatory factors and causing cell cycle arrest in spermatogenic cells. *Environ Sci Pollut Res Int* 23:20506–20516. doi:10.1007/s11356-016-7195-y
- Hiruma K et al (2013) Glutathione and tryptophan metabolism are required for *Arabidopsis* immunity during the hypersensitive response to hemibiotrophs. *Proc Natl Acad Sci U S A* 110:9589–9594. doi:10.1073/pnas.1305745110
- Jia H et al (2010) Monitoring and modeling endosulfan in Chinese surface soil. *Environ Sci Technol* 44:9279–9284. doi:10.1021/es102791n
- Jobgen WS, Fried SK, Fu WJ, Meininger CJ, Wu G (2006) Regulatory role for the arginine-nitric oxide pathway in metabolism of energy substrates. *J Nutr Biochem* 17:571–588. doi:10.1016/j.jnutbio.2005.12.001
- Kalender S, Kalender Y, Ogutcu A, Uzunhisarcikli M, Durak D, Acikgoz F (2004) Endosulfan-induced cardiotoxicity and free radical metabolism in rats: the protective effect of vitamin E. *Toxicology* 202:227–235. doi:10.1016/j.tox.2004.05.010
- Kaspar H (2009) Amino acid analysis in biological fluids by GC-MS. Dissertation, University of Regensburg
- Kohlmeier M, da Costa KA, Fischer LM, Zeisel SH (2005) Genetic variation of folate-mediated one-carbon transfer pathway predicts susceptibility to choline deficiency in humans. *Proc Natl Acad Sci U S A* 102:16025–16030. doi:10.1073/pnas.0504285102
- Landfried K et al (2011) Tryptophan catabolism is associated with acute GVHD after human allogeneic stem cell transplantation and indicates activation of indoleamine 2,3-dioxygenase. *Blood* 118:6971–6974. doi:10.1182/blood-2011-06-357814
- Li YF, Macdonald RW (2005) Sources and pathways of selected organochlorine pesticides to the Arctic and the effect of pathway divergence on HCH trends in biota: a review. *Sci Total Environ* 342:87–106. doi:10.1016/j.scitotenv.2004.12.027
- Li Z, Agellon LB, Vance DE (2005) Phosphatidylcholine homeostasis and liver failure. *J Biol Chem* 280:37798–37802. doi:10.1074/jbc.M508575200
- Li H, An Y, Zhang L, Lei H, Wang Y, Tang H (2013) Combined NMR and GC-MS analyses revealed dynamic metabolic changes associated with the carrageenan-induced rat pleurisy. *J Proteome Res* 12:5520–5534. doi:10.1021/pr400440d
- Lu Y, Morimoto K, Takeshita T, Takeuchi T, Saito T (2000) Genotoxic effects of alpha-endosulfan and beta-endosulfan on human HepG2 cells. *Environ Health Perspect* 108:559–561. doi:10.2307/3454619
- Machala M et al (2004) Toxicity of hydroxylated and quinoid PCB metabolites: inhibition of gap junctional intercellular communication and activation of aryl hydrocarbon and estrogen receptors in hepatic and mammary cells. *Chem Res Toxicol* 17:340–347. doi:10.1021/tx030034v
- Mannick JB (2007) Regulation of apoptosis by protein S-nitrosylation. *Amino Acids* 32:523–526. doi:10.1007/s00726-006-0427-6
- Marc Rhoads J, Wu G (2009) Glutamine, arginine, and leucine signaling in the intestine. *Amino Acids* 37:111–122. doi:10.1007/s00726-008-0225-4
- McCombie G, Browning LM, Titman CM, Song M, Shockcor J, Jebb SA, Griffin JL (2009) Omega-3 oil intake during weight loss in obese women results in remodelling of plasma triglyceride and fatty acids metabolomics. *Metabolomics* 5:363–374. doi:10.1007/s11306-009-0161-7
- Mehrmohamadi M, Liu X, Shestov AA, Locasale JW (2014) Characterization of the usage of the serine metabolic network in human cancer. *Cell Rep* 9:1507–1519. doi:10.1016/j.celrep.2014.10.026
- Meijer AJ (2003) Amino acids as regulators and components of nonproteinogenic pathways. *J Nutr* 133:2057S–2062S
- Noel M, Loseto LL, Helbing CC, Veldhoen N, Dangerfield NJ, Ross PS (2014) PCBs are associated with altered gene transcript profiles in arctic beluga whales (*Delphinapterus leucas*). *Environ Sci Technol* 48:2942–2951. doi:10.1021/es403217r
- Nomiyama K et al (2014) Toxicological assessment of polychlorinated biphenyls and their metabolites in the liver of Baikal seal (*Pusa sibirica*). *Environ Sci Technol* 48:13530–13539. doi:10.1021/es5043386
- Pereira VM et al (2012) Endosulfan exposure inhibits brain AChE activity and impairs swimming performance in adult zebrafish (*Danio rerio*). *Neurotoxicology* 33:469–475. doi:10.1016/j.neuro.2012.03.005
- Quinete N, Castro J, Fernandez A, Zamora-Ley IM, Rand GM, Gardinali PR (2013) Occurrence and distribution of endosulfan in water, sediment, and fish tissue: an ecological assessment of protected lands in south Florida. *J Agric Food Chem* 61:11881–11892. doi:10.1021/jf403140z

- Schmidt WF et al (2014) Temperature-dependent Raman spectroscopic evidence of and molecular mechanism for irreversible isomerization of beta-endosulfan to alpha-endosulfan. *J Agric Food Chem* 62: 2023–2030. doi:10.1021/jf404404w
- Shao B et al (2012) DNA damage and oxidative stress induced by endosulfan exposure in zebrafish (*Danio rerio*). *Ecotoxicology* 21:1533–1540. doi:10.1007/s10646-012-0907-2
- Shi X et al (2012) Metabolomic analysis of the effects of polychlorinated biphenyls in nonalcoholic fatty liver disease. *J Proteome Res* 11: 3805–3815. doi:10.1021/pr300297z
- Silva MH, Beauvais SL (2010) Human health risk assessment of endosulfan. I: Toxicology and hazard identification. *Regul Toxicol Pharmacol*: RTP 56:4–17. doi:10.1016/j.yrtph.2009.08.013
- Sohn HY, Kwon CS, Kwon GS, Lee JB, Kim E (2004) Induction of oxidative stress by endosulfan and protective effect of lipid-soluble antioxidants against endosulfan-induced oxidative damage. *Toxicol Lett* 151:357–365. doi:10.1016/j.toxlet.2004.03.004
- Song X et al (2015) Polychlorinated biphenyl quinone metabolite promotes p53-dependent DNA damage checkpoint activation, S-phase cycle arrest and extrinsic apoptosis in human liver hepatocellular carcinoma HepG2 cells. *Chem Res Toxicol*. doi:10.1021/acs.chemrestox.5b00320
- Stanley KA, Curtis LR, Simonich SL, Tanguay RL (2009) Endosulfan I and endosulfan sulfate disrupts zebrafish embryonic development. *Aquat Toxicol* 95:355–361. doi:10.1016/j.aquatox.2009.10.008
- Trousil S et al (2014) Alterations of choline phospholipid metabolism in endometrial cancer are caused by choline kinase alpha overexpression and a hyperactivated deacylation pathway. *Cancer Res* 74: 6867–6877. doi:10.1158/0008-5472.can-13-2409
- Tyagi R et al (2012) Urinary metabolomic phenotyping of nickel induced acute toxicity in rat: an NMR spectroscopy approach. *Metabolomics* 8:940–950. doi:10.1007/s11306-011-0390-4
- Uboh FE, Asuquo EN, Eteng MU (2011) Endosulfan-induced hepatotoxicity is route of exposure independent in rats. *Toxicol Ind Health* 27: 483–488. doi:10.1177/0748233710387011
- van der Goot AT et al (2012) Delaying aging and the aging-associated decline in protein homeostasis by inhibition of tryptophan degradation. *Proc Natl Acad Sci U S A* 109:14912–14917. doi:10.1073/pnas.1203083109
- Wang LF et al (2012) Application of <sup>1</sup>H-NMR-based metabolomics for detecting injury induced by long-term microwave exposure in Wistar rats' urine. *Anal Bioanal Chem* 404:69–78. doi:10.1007/s00216-012-6115-3
- Weber J et al (2010) Endosulfan, a global pesticide: a review of its fate in the environment and occurrence in the Arctic. *Sci Total Environ* 408:2966–2984. doi:10.1016/j.scitotenv.2009.10.077
- Wu G (2009) Amino acids: metabolism, functions, and nutrition. *Amino Acids* 37:1–17. doi:10.1007/s00726-009-0269-0
- Wu G, Fang YZ, Yang S, Lupton JR, Turner ND (2004) Glutathione metabolism and its implications for health. *J Nutr* 134:489–492
- Xu J, Jiang H, Li J, Cheng KK, Dong J, Chen Z (2015) <sup>1</sup>H NMR-based metabolomics investigation of copper-laden rat: a model of Wilson's disease. *PLoS One* 10:e0119654. doi:10.1371/journal.pone.0119654
- Yuk J, Simpson MJ, Simpson AJ (2013) 1-D and 2-D NMR-based metabolomics of earthworms exposed to endosulfan and endosulfan sulfate in soil. *Environ Pollut* 175:35–44. doi:10.1016/j.envpol.2012.12.007
- Zeisel SH (2011) Nutritional genomics: defining the dietary requirement and effects of choline. *J Nutr* 141:531–534. doi:10.3945/jn.110.130369
- Zhang L, Ye Y, An Y, Tian Y, Wang Y, Tang H (2011) Systems responses of rats to aflatoxin B1 exposure revealed with metabolomic changes in multiple biological matrices. *J Proteome Res* 10:614–623. doi:10.1021/pr100792q
- Zhang Y, Zhang Z, Zhao Y, Cheng S, Ren H (2013) Identifying health effects of exposure to trichloroacetamide using transcriptomics and metabolomics in mice (*Mus musculus*). *Environ Sci Technol* 47: 2918–2924. doi:10.1021/es3048976
- Zhang L et al (2014) Metabonomic analysis reveals efficient ameliorating effects of acupoint stimulations on the menopause-caused alterations in mammalian metabolism. *Sci Rep* 4:3641. doi:10.1038/srep03641
- Zhang L et al (2015a) Metabolomics reveals that aryl hydrocarbon receptor activation by environmental chemicals induces systemic metabolic dysfunction in mice. *Environ Sci Technol* 49:8067–8077. doi:10.1021/acs.est.5b01389
- Zhang Y, Zhao F, Deng Y, Zhao Y, Ren H (2015b) Metagenomic and metabolomic analysis of the toxic effects of trichloroacetamide-induced gut microbiome and urine metabolome perturbations in mice. *J Proteome Res* 14:1752–1761. doi:10.1021/pr5011263
- Zhu W et al (2011) Quantitative profiling of tryptophan metabolites in serum, urine, and cell culture supernatants by liquid chromatography-tandem mass spectrometry. *Anal Bioanal Chem* 401:3249–3261. doi:10.1007/s00216-011-5436-y
- Zhu J, Wu Y, Tang Q, Leng Y, Cai W (2014) The effects of choline on hepatic lipid metabolism, mitochondrial function and antioxidative status in human hepatic C3A cells exposed to excessive energy substrates. *Nutrients* 6:2552–2571. doi:10.3390/nu6072552